

Measurement of $\mathcal{B}(\psi(3770) \rightarrow \gamma\chi_{c1})$ and search for $\psi(3770) \rightarrow \gamma\chi_{c2}$

M. Ablikim¹, M. N. Achasov^{9,a}, X. C. Ai¹, O. Albayrak⁵, M. Albrecht⁴, D. J. Ambrose⁴⁴, A. Amoroso^{48A,48C}, F. F. An¹, Q. An⁴⁵, J. Z. Bai¹, R. Baldini Ferroli^{20A}, Y. Ban³¹, D. W. Bennett¹⁹, J. V. Bennett⁵, M. Bertani^{20A}, D. Bettoni^{21A}, J. M. Bian⁴³, F. Bianchi^{48A,48C}, E. Boger^{23,h}, O. Bondarenko²⁵, I. Boyko²³, R. A. Briere⁵, H. Cai⁵⁰, X. Cai¹, O. Cakir^{40A,b}, A. Calcaterra^{20A}, G. F. Cao¹, S. A. Cetin^{40B}, J. F. Chang¹, G. Chelkov^{23,c}, G. Chen¹, H. S. Chen¹, H. Y. Chen², J. C. Chen¹, M. L. Chen¹, S. J. Chen²⁹, X. Chen¹, X. R. Chen²⁶, Y. B. Chen¹, H. P. Cheng¹⁷, X. K. Chu³¹, G. Cibinetto^{21A}, D. Cronin-Hennessy⁴³, H. L. Dai¹, J. P. Dai³⁴, A. Dbeysli¹⁴, D. Dedovich²³, Z. Y. Deng¹, A. Denig²², I. Denysenko²³, M. Destefanis^{48A,48C}, F. De Mori^{48A,48C}, Y. Ding²⁷, C. Dong³⁰, J. Dong¹, L. Y. Dong¹, M. Y. Dong¹, S. X. Du⁵², P. F. Duan¹, J. Z. Fan³⁹, J. Fang¹, S. S. Fang¹, X. Fang⁴⁵, Y. Fang¹, L. Fava^{48B,48C}, F. Feldbauer²², G. Felici^{20A}, C. Q. Feng⁴⁵, E. Fioravanti^{21A}, M. Fritsch^{14,22}, C. D. Fu¹, Q. Gao¹, X. Y. Gao², Y. Gao³⁹, Z. Gao⁴⁵, I. Garzia^{21A}, C. Geng⁴⁵, K. Goetzen¹⁰, W. X. Gong¹, W. Grad²², M. Greco^{48A,48C}, M. H. Gu¹, Y. T. Gu¹², Y. H. Guan¹, A. Q. Guo¹, L. B. Guo²⁸, Y. Guo¹, Y. P. Guo²², Z. Haddadi²⁵, A. Hafner²², S. Han⁵⁰, Y. L. Han¹, X. Q. Hao¹⁵, F. A. Harris⁴², K. L. He¹, Z. Y. He³⁰, T. Held⁴, Y. K. Heng¹, Z. L. Hou¹, C. Hu²⁸, H. M. Hu¹, J. F. Hu^{48A,48C}, T. Hu¹, Y. Hu¹, G. M. Huang⁶, G. S. Huang⁴⁵, H. P. Huang⁵⁰, J. S. Huang¹⁵, X. T. Huang³³, Y. Huang²⁹, T. Hussain⁴⁷, Q. Ji¹, Q. P. Ji³⁰, X. B. Ji¹, X. L. Ji¹, L. L. Jiang¹, L. W. Jiang⁵⁰, X. S. Jiang¹, J. B. Jiao³³, Z. Jiao¹⁷, D. P. Jin¹, S. Jin¹, T. Johansson⁴⁹, A. Julin⁴³, N. Kalantar-Nayestanaki²⁵, X. L. Kang¹, X. S. Kang³⁰, M. Kavatsyuk²⁵, B. C. Ke⁵, R. Kliemt¹⁴, B. Kloss²², O. B. Kolcu^{40B,d}, B. Kopf⁴, M. Kornicer⁴², W. Kühn²⁴, A. Kupsc⁴⁹, W. Lai¹, J. S. Lange²⁴, M. Lara¹⁹, P. Larin¹⁴, C. Leng^{48C}, C. H. Li¹, Cheng Li⁴⁵, D. M. Li⁵², F. Li¹, G. Li¹, H. B. Li¹, J. C. Li¹, Jin Li³², K. Li¹³, K. Li³³, Lei Li³, P. R. Li⁴¹, T. Li³³, W. D. Li¹, W. G. Li¹, X. L. Li³³, X. M. Li¹², X. N. Li¹, X. Q. Li³⁰, Z. B. Li³⁸, H. Liang⁴⁵, Y. F. Liang³⁶, Y. T. Liang²⁴, G. R. Liao¹¹, D. X. Lin¹⁴, B. J. Liu¹, C. X. Liu¹, F. H. Liu³⁵, Fang Liu¹, Feng Liu⁶, H. B. Liu¹², H. H. Liu¹, H. H. Liu¹⁶, H. M. Liu¹, J. Liu¹, J. P. Liu⁵⁰, J. Y. Liu¹, K. Liu³⁹, K. Y. Liu²⁷, L. D. Liu³¹, P. L. Liu¹, Q. Liu⁴¹, S. B. Liu⁴⁵, X. Liu²⁶, X. X. Liu⁴¹, Y. B. Liu³⁰, Z. A. Liu¹, Zhiqiang Liu¹, Zhiqing Liu²², H. Loehner²⁵, X. C. Lou^{1,e}, H. J. Lu¹⁷, J. G. Lu¹, R. Q. Lu¹⁸, Y. Lu¹, Y. P. Lu¹, C. L. Luo²⁸, M. X. Luo⁵¹, T. Luo⁴², X. L. Luo¹, M. Lv¹, X. R. Lyu⁴¹, F. C. Ma²⁷, H. L. Ma¹, L. L. Ma³³, Q. M. Ma¹, S. Ma¹, T. Ma¹, X. N. Ma³⁰, X. Y. Ma¹, F. E. Maas¹⁴, M. Maggiora^{48A,48C}, Q. A. Malik⁴⁷, Y. J. Mao³¹, Z. P. Mao¹, S. Marcello^{48A,48C}, J. G. Messchendorp²⁵, J. Min¹, T. J. Min¹, R. E. Mitchell¹⁹, X. H. Mo¹, Y. J. Mo⁶, C. Morales Morales¹⁴, K. Moriya¹⁹, N. Yu. Muchnoi^{9,a}, H. Muramatsu⁴³, Y. Nefedov²³, F. Nerling¹⁴, I. B. Nikolaev^{9,a}, Z. Ning¹, S. Nisar⁸, S. L. Niu¹, X. Y. Niu¹, S. L. Olsen³², Q. Ouyang¹, S. Pacetti^{20B}, P. Patteri^{20A}, M. Pelizaeus⁴, H. P. Peng⁴⁵, K. Peters¹⁰, J. Pettersson⁴⁹, J. L. Ping²⁸, R. G. Ping¹, R. Poling⁴³, Y. N. Pu¹⁸, M. Qi²⁹, S. Qian¹, C. F. Qiao⁴¹, L. Q. Qin³³, N. Qin⁵⁰, X. S. Qin¹, Y. Qin³¹, Z. H. Qin¹, J. F. Qiu¹, K. H. Rashid⁴⁷, C. F. Redmer²², H. L. Ren¹⁸, M. Ripka²², G. Rong¹, X. D. Ruan¹², V. Santoro^{21A}, A. Sarantsev^{23,f}, M. Savrié^{21B}, K. Schoenning⁴⁹, S. Schumann²², W. Shan³¹, M. Shao⁴⁵, C. P. Shen², P. X. Shen³⁰, X. Y. Shen¹, H. Y. Sheng¹, W. M. Song¹, X. Y. Song¹, S. Sosio^{48A,48C}, S. Spataro^{48A,48C}, G. X. Sun¹, J. F. Sun¹⁵, S. S. Sun¹, Y. J. Sun⁴⁵, Y. Z. Sun¹, Z. J. Sun¹, Z. T. Sun¹⁹, C. J. Tang³⁶, X. Tang¹, I. Tapan^{40C}, E. H. Thorndike⁴⁴, M. Tiemens²⁵, D. Toth⁴³, M. Ullrich²⁴, I. Uman^{40B}, G. S. Varner⁴², B. Wang³⁰, B. L. Wang⁴¹, D. Wang³¹, D. Y. Wang³¹, K. Wang¹, L. L. Wang¹, L. S. Wang¹, M. Wang³³, P. Wang¹, P. L. Wang¹, Q. J. Wang¹, S. G. Wang³¹, W. Wang¹, X. F. Wang³⁹, Y. D. Wang^{20A}, Y. F. Wang¹, Y. Q. Wang²², Z. Wang¹, Z. G. Wang¹, Z. H. Wang⁴⁵, Z. Y. Wang¹, T. Weber²², D. H. Wei¹¹, J. B. Wei³¹, P. Weidenkaff²², S. P. Wen¹, U. Wiedner⁴, M. Wolke⁴⁹, L. H. Wu¹, Z. Wu¹, L. G. Xia³⁹, Y. Xia¹⁸, D. Xiao¹, Z. J. Xiao²⁸, Y. G. Xie¹, Q. L. Xiu¹, G. F. Xu¹, L. Xu¹, Q. J. Xu¹³, Q. N. Xu⁴¹, X. P. Xu³⁷, L. Yan⁴⁵, W. B. Yan⁴⁵, W. C. Yan⁴⁵, Y. H. Yan¹⁸, H. X. Yang¹, L. Yang⁵⁰, C. Z. Yuan⁶, Y. X. Yang¹¹, H. Ye¹, M. Ye¹, M. H. Ye⁷, J. H. Yin¹, B. X. Yu¹, C. X. Yu³⁰, H. W. Yu³¹, J. S. Yu²⁶, C. Z. Yuan¹, W. L. Yuan²⁹, Y. Yuan¹, A. Yuncu^{40B,g}, A. A. Zafar⁴⁷, A. Zallo^{20A}, Y. Zeng¹⁸, B. X. Zhang¹, B. Y. Zhang¹, C. Zhang²⁹, C. C. Zhang¹, D. H. Zhang¹, H. H. Zhang³⁸, H. Y. Zhang¹, J. J. Zhang¹, J. L. Zhang¹, J. Q. Zhang¹, J. W. Zhang¹, J. Y. Zhang¹, J. Z. Zhang¹, K. Zhang¹, L. Zhang¹, S. H. Zhang¹, X. Y. Zhang³³, Y. Zhang¹, Y. H. Zhang¹, Y. T. Zhang⁴⁵, Z. H. Zhang⁶, Z. P. Zhang⁴⁵, Z. Y. Zhang⁵⁰, G. Zhao¹, J. W. Zhao¹, J. Y. Zhao¹, J. Z. Zhao¹, Lei Zhao⁴⁵, Ling Zhao¹, M. G. Zhao³⁰, Q. Zhao¹, Q. W. Zhao¹, S. J. Zhao⁵², T. C. Zhao¹, Y. B. Zhao¹, Z. G. Zhao⁴⁵, A. Zhemchugov^{23,h}, B. Zheng⁴⁶, J. P. Zheng¹, W. J. Zheng³³, Y. H. Zheng⁴¹, B. Zhong²⁸, L. Zhou¹, Li Zhou³⁰, X. Zhou⁵⁰, X. K. Zhou⁴⁵, X. R. Zhou⁴⁵, X. Y. Zhou¹, K. Zhu¹, K. J. Zhu¹, S. Zhu¹, X. L. Zhu³⁹, Y. C. Zhu⁴⁵, Y. S. Zhu¹, Z. A. Zhu¹, J. Zhuang¹, L. Zotti^{48A,48C}, B. S. Zou¹, J. H. Zou¹

(BESIII Collaboration)

¹ Institute of High Energy Physics, Beijing 100049, People's Republic of China

² Beihang University, Beijing 100191, People's Republic of China

³ Beijing Institute of Petrochemical Technology, Beijing 102617, People's Republic of China

⁴ Bochum Ruhr-University, D-44780 Bochum, Germany

⁵ Carnegie Mellon University, Pittsburgh, Pennsylvania 15213, USA

⁶ Central China Normal University, Wuhan 430079, People's Republic of China

⁷ China Center of Advanced Science and Technology, Beijing 100190, People's Republic of China

⁸ COMSATS Institute of Information Technology, Lahore, Defence Road, Off Raiwind Road, 54000 Lahore, Pakistan

⁹ G.I. Budker Institute of Nuclear Physics SB RAS (BINP), Novosibirsk 630090, Russia

¹⁰ GSI Helmholtzcentre for Heavy Ion Research GmbH, D-64291 Darmstadt, Germany

¹¹ Guangxi Normal University, Guilin 541004, People's Republic of China

¹² GuangXi University, Nanning 530004, People's Republic of China

¹³ Hangzhou Normal University, Hangzhou 310036, People's Republic of China

- ¹⁴ *Helmholtz Institute Mainz, Johann-Joachim-Becher-Weg 45, D-55099 Mainz, Germany*
- ¹⁵ *Henan Normal University, Xinxiang 453007, People's Republic of China*
- ¹⁶ *Henan University of Science and Technology, Luoyang 471003, People's Republic of China*
- ¹⁷ *Huangshan College, Huangshan 245000, People's Republic of China*
- ¹⁸ *Hunan University, Changsha 410082, People's Republic of China*
- ¹⁹ *Indiana University, Bloomington, Indiana 47405, USA*
- ²⁰ (A)*INFN Laboratori Nazionali di Frascati, I-00044, Frascati, Italy; (B)INFN and University of Perugia, I-06100, Perugia, Italy*
- ²¹ (A)*INFN Sezione di Ferrara, I-44122, Ferrara, Italy; (B)University of Ferrara, I-44122, Ferrara, Italy*
- ²² *Johannes Gutenberg University of Mainz, Johann-Joachim-Becher-Weg 45, D-55099 Mainz, Germany*
- ²³ *Joint Institute for Nuclear Research, 141980 Dubna, Moscow region, Russia*
- ²⁴ *Justus Liebig University Giessen, II. Physikalisches Institut, Heinrich-Buff-Ring 16, D-35392 Giessen, Germany*
- ²⁵ *KVI-CART, University of Groningen, NL-9747 AA Groningen, Netherlands*
- ²⁶ *Lanzhou University, Lanzhou 730000, People's Republic of China*
- ²⁷ *Liaoning University, Shenyang 110036, People's Republic of China*
- ²⁸ *Nanjing Normal University, Nanjing 210023, People's Republic of China*
- ²⁹ *Nanjing University, Nanjing 210093, People's Republic of China*
- ³⁰ *Nankai University, Tianjin 300071, People's Republic of China*
- ³¹ *Peking University, Beijing 100871, People's Republic of China*
- ³² *Seoul National University, Seoul, 151-747 Korea*
- ³³ *Shandong University, Jinan 250100, People's Republic of China*
- ³⁴ *Shanghai Jiao Tong University, Shanghai 200240, People's Republic of China*
- ³⁵ *Shanxi University, Taiyuan 030006, People's Republic of China*
- ³⁶ *Sichuan University, Chengdu 610064, People's Republic of China*
- ³⁷ *Soochow University, Suzhou 215006, People's Republic of China*
- ³⁸ *Sun Yat-Sen University, Guangzhou 510275, People's Republic of China*
- ³⁹ *Tsinghua University, Beijing 100084, People's Republic of China*
- ⁴⁰ (A)*Istanbul Aydin University, 34295 Sefakoy, Istanbul, Turkey; (B)Dogus University, 34722 Istanbul, Turkey; (C)Uludag University, 16059 Bursa, Turkey*
- ⁴¹ *University of Chinese Academy of Sciences, Beijing 100049, People's Republic of China*
- ⁴² *University of Hawaii, Honolulu, Hawaii 96822, USA*
- ⁴³ *University of Minnesota, Minneapolis, Minnesota 55455, USA*
- ⁴⁴ *University of Rochester, Rochester, New York 14627, USA*
- ⁴⁵ *University of Science and Technology of China, Hefei 230026, People's Republic of China*
- ⁴⁶ *University of South China, Hengyang 421001, People's Republic of China*
- ⁴⁷ *University of the Punjab, Lahore-54590, Pakistan*
- ⁴⁸ (A)*University of Turin, I-10125, Turin, Italy; (B)University of Eastern Piedmont, I-15121, Alessandria, Italy; (C)INFN, I-10125, Turin, Italy*
- ⁴⁹ *Uppsala University, Box 516, SE-75120 Uppsala, Sweden*
- ⁵⁰ *Wuhan University, Wuhan 430072, People's Republic of China*
- ⁵¹ *Zhejiang University, Hangzhou 310027, People's Republic of China*
- ⁵² *Zhengzhou University, Zhengzhou 450001, People's Republic of China*
- ^a *Also at the Novosibirsk State University, Novosibirsk, 630090, Russia*
- ^b *Also at Ankara University, 06100 Tandogan, Ankara, Turkey*
- ^c *Also at the Moscow Institute of Physics and Technology, Moscow 141700, Russia and at the Functional Electronics Laboratory, Tomsk State University, Tomsk, 634050, Russia*
- ^d *Currently at Istanbul Arel University, 34295 Istanbul, Turkey*
- ^e *Also at University of Texas at Dallas, Richardson, Texas 75083, USA*
- ^f *Also at the NRC "Kurchatov Institute", PNPI, 188300, Gatchina, Russia*
- ^g *Also at Bogazici University, 34342 Istanbul, Turkey*
- ^h *Also at the Moscow Institute of Physics and Technology, Moscow 141700, Russia*

(Dated: October 26, 2021)

We report a measurement of the branching fraction for $\psi(3770) \rightarrow \gamma\chi_{c1}$ and search for the transition $\psi(3770) \rightarrow \gamma\chi_{c2}$ based on 2.92 fb^{-1} of e^+e^- data accumulated at $\sqrt{s} = 3.773 \text{ GeV}$ with the BESIII detector at the BEPCII collider. We measure $\mathcal{B}(\psi(3770) \rightarrow \gamma\chi_{c1}) = (2.48 \pm 0.15 \pm 0.23) \times 10^{-3}$, which is the most precise measurement to date. The upper limit on the branching fraction of $\psi(3770) \rightarrow \gamma\chi_{c2}$ at a 90% confidence level is $\mathcal{B}(\psi(3770) \rightarrow \gamma\chi_{c2}) < 0.64 \times 10^{-3}$. The corresponding partial widths are $\Gamma(\psi(3770) \rightarrow \gamma\chi_{c1}) = (67.5 \pm 4.1 \pm 6.7) \text{ keV}$ and $\Gamma(\psi(3770) \rightarrow \gamma\chi_{c2}) < 17.4 \text{ keV}$.

PACS numbers: 14.40.Pq, 13.20.Gd

I. INTRODUCTION

The $\psi(3770)$ resonance is the lowest-mass $c\bar{c}$ state lying above the open charm-pair threshold ($3.73 \text{ GeV}/c^2$). Since its width is 2 orders of magnitude larger than that of the $\psi(3686)$ resonance, it is traditionally expected to decay to $D\bar{D}$ meson pairs with a branching fraction of more than 99% [1]. This would be consistent with other conventional mesons lying in the energy region between the open-charm and open-bottom thresholds. However, if a meson lying in this region contains not only a $c\bar{c}$ pair but also a number of constituent gluons or additional light quarks and antiquarks, it may more easily decay to non- $D\bar{D}$ final states (such as a lower-mass $c\bar{c}$ pair plus pions [2] or light hadrons [3]) than conventional mesons. In addition, if there are some unknown conventional or unconventional mesons nearby the $c\bar{c}$ state under study, the measured non-open-charm-pair decay branching fraction of the $c\bar{c}$ state could also be large [4]. For this reason, searching for non-open-charm-pair decays of the mesons lying in this region has become a way to search for unconventional mesons.

In 2003, the BES Collaboration found the first non-open-charm-pair final state of $J/\psi\pi^+\pi^-$ [5, 6] in data taken at 3.773 GeV. Since the final state $J/\psi\pi^+\pi^-$ cannot be directly produced in e^+e^- annihilation, this process is interpreted to be a hadronic transition $\psi(3770) \rightarrow J/\psi\pi^+\pi^-$, although it has not been excluded that this final state may be a decay product of some other possible structures [7] which may exist in this energy region. Following this observation, the CLEO Collaboration found that $\psi(3770)$ can also decay into $J/\psi\pi^0\pi^0$, $J/\psi\eta$ [8], $\gamma\chi_{c0}$ [9], $\gamma\chi_{c1}$ [10] and $\phi\eta$ [11]. In the CLEO-c measurements, the χ_{c0} and χ_{c1} were reconstructed with $\chi_{c0} \rightarrow$ light hadrons and $\chi_{c1} \rightarrow \gamma J/\psi$, respectively. These observations stimulate strong interest in studying other non- $D\bar{D}$ decays of the $\psi(3770)$, as well as searching for non-open-charm-pair decays of other mesons lying in the energy region between the open charm-pair and open bottom-pair thresholds, particularly searching for $J/\psi X$ or $c\bar{c}X$ (where X denotes any other particle, or $n\pi$, nK , and η , where $n = 1, 2, 3 \dots$) decays of these mesons in this energy region.

Within an S - D mixing model, the $\psi(3770)$ resonance is assumed to be predominantly the 1^3D_1 $c\bar{c}$ state with a small admixture of the 2^3S_1 state. Based on this assumption, Refs. [12–15] predict the partial widths of $\psi(3770)$ $E1$ radiative transitions, but with large uncertainties. For example, the partial widths for $\psi(3770) \rightarrow \gamma\chi_{c1}$ and $\psi(3770) \rightarrow \gamma\chi_{c2}$ range from 59 to 183 keV and from 3 to 24 keV, respectively. In addition, the transition $\psi(3770) \rightarrow \gamma\chi_{c2}$ has yet to be observed. Therefore, precision measurements of partial widths of the $\psi(3770) \rightarrow \gamma\chi_{c1,2}$ processes are critical to test the above mentioned models, and to better understand the nature of the $\psi(3770)$, as well as to find the origin of the non- $D\bar{D}$ decays of the $\psi(3770)$.

In this paper, we report a measurement of the branch-

ing fraction for the transition $\psi(3770) \rightarrow \gamma\chi_{c1}$ and search for the transition $\psi(3770) \rightarrow \gamma\chi_{c2}$ based on $(2916.94 \pm 29.17) \text{ pb}^{-1}$ of e^+e^- data [16] taken at $\sqrt{s} = 3.773 \text{ GeV}$ with the BESIII detector [17] operated at the BEPCII collider.

II. BESIII DETECTOR

The BESIII [17] detector is a cylindrical detector with a solid-angle coverage of 93% of 4π that operates at the BEPCII [17] e^+e^- collider. It consists of several main components. A 43-layer main drift chamber (MDC) surrounding the beam pipe performs precise determinations of charged particle trajectories and provides ionization energy loss (dE/dx) measurements that are used for charged-particle identification. An array of time-of-flight counters (TOF) is located radially outside of the MDC and provides additional charged particle identification information. The time resolution of the TOF system is 80 ps (110 ps) in the barrel (end-cap) regions, corresponding to better than 2σ K/π separation for momenta below about 1 GeV/c. The solid angle coverage of the barrel TOF is $|\cos\theta| < 0.83$, while that of the end cap is $0.85 < |\cos\theta| < 0.95$, where θ is the polar angle. A CsI(Tl) electromagnetic calorimeter (EMC) surrounds the TOF and is used to measure the energies of photons and electrons. The angular coverage of the barrel EMC is $|\cos\theta| < 0.82$. The two end caps cover $0.83 < |\cos\theta| < 0.93$. A solenoidal superconducting magnet located outside the EMC provides a 1 T magnetic field in the central tracking region of the detector. The iron flux return of the magnet is instrumented with about 1200 m² of resistive plate muon counters (MUC) arranged in nine layers in the barrel and eight layers in the end caps that are used to identify muons with momentum greater than 500 MeV/c.

The BESIII detector response is studied using samples of Monte Carlo (MC) simulated events which are simulated with a GEANT4-based [18] detector simulation software package, BOOST [19]. The production of the $\psi(3770)$ resonance is simulated with the Monte Carlo event generator \mathcal{KK} , KKMC [20]. The decays of $\psi(3770) \rightarrow \gamma\chi_{cJ}$ ($J = 0, 1, 2$) are generated with EVTGEN [21] according to the expected angular distributions [22]. In order to study possible backgrounds, Monte Carlo samples of inclusive $\psi(3770)$ decays, $e^+e^- \rightarrow (\gamma)J/\psi$, $e^+e^- \rightarrow (\gamma)\psi(3686)$, and $e^+e^- \rightarrow q\bar{q}$ ($q = u, d, s$) are also generated. For inclusive decays of $\psi(3770)$, $\psi(3686)$ and J/ψ , the known decay modes are generated by EVTGEN with branching fractions taken from the PDG [23], while the remaining unknown decay modes are modeled by LUNDCHARM [24]. In addition, the background process $e^+e^- \rightarrow \tau^+\tau^-$ is generated with KKMC, while the backgrounds from $e^+e^- \rightarrow (\gamma)e^+e^-$ and $e^+e^- \rightarrow (\gamma)\mu^+\mu^-$ are generated with the generator BABAYAGA [25].

III. ANALYSIS

In this analysis, the process $\psi(3770) \rightarrow \gamma\chi_{cJ}$ ($J = 1, 2$) is reconstructed using the decay chain $\chi_{cJ} \rightarrow \gamma J/\psi$, $J/\psi \rightarrow \ell^+\ell^-$ ($\ell = e$ or μ).

A. Event selection

Events that contain two good photon candidates and exactly two oppositely charged tracks are selected for further analysis. For the selection of photons, the deposited energy of a neutral cluster in the EMC is required to be greater than 50 MeV. Time information from the EMC is used to suppress electronic noise and energy deposits unrelated to the event. To exclude false photons originating from charged tracks, the angle between the photon candidate and the nearest charged track is required to be greater than 10° . Charged tracks are reconstructed from hit patterns in the MDC. For each charged track, the polar angle θ is required to satisfy $|\cos\theta| < 0.93$. All charged tracks are required to have a distance of closest approach to the average e^+e^- interaction point that is less than 1.0 cm in the plane perpendicular to the beam and less than 15.0 cm along the beam direction. Electron and muon candidates can be well separated with the ratio E/p , where E is the energy deposited in the EMC and p is the momentum measured in the MDC. If the ratio E/p is greater than 0.7, the charged track is identified as an electron or positron. Otherwise, if the energy deposited in the EMC is in the range from 0.05 to 0.35 GeV, the charged track is identified as a muon. The J/ψ candidates are reconstructed from pairs of leptons with momenta in a range from 1.2 to 1.9 GeV/ c .

In the selection of the $\gamma\gamma e^+e^-$ mode, we further require that the cosine of the polar angle of the positron and electron, θ_{e^+} and θ_{e^-} , satisfy $\cos\theta_{e^+} < 0.5$ and $\cos\theta_{e^-} > -0.5$ to reduce the number of background events from radiative Bhabha scattering.

To exclude background events from $J/\psi\pi^0$ and $J/\psi\eta$ with $\pi^0 \rightarrow \gamma\gamma$ and $\eta \rightarrow \gamma\gamma$, the invariant mass of the two photons is required to be outside of the π^0 mass window (0.124, 0.146) GeV/ c^2 and the η mass window (0.537, 0.558) GeV/ c^2 .

B. Kinematic fit and mass spectrum of $\gamma J/\psi$

In order to both reduce background and improve the mass resolution, a kinematic fit is performed under the $\gamma\gamma\ell^+\ell^-$ hypothesis. We constrain the total energy and the components of the total momentum to the expected center-of-mass energy and the three-momentum, taking into account the small beam crossing angle. In addition to these, we constrain the invariant mass of the $\ell^+\ell^-$ pair to the J/ψ mass. If the χ^2 of the 5-constraint (5C) kinematic fit is less than 25, the event is kept for further analysis.

The energy of the γ from the transition $\psi(3770) \rightarrow \gamma\chi_{cJ}$ for $J = 1, 2$ is lower than that of the γ from the subsequent transition $\chi_{cJ} \rightarrow \gamma J/\psi$, while the energy of the γ from the transition $\psi(3770) \rightarrow \gamma\chi_{c0}$ is usually higher than that of the γ from the subsequent transition $\chi_{c0} \rightarrow \gamma J/\psi$. To reconstruct the χ_{c1} and χ_{c2} from the radiative decay of the $\psi(3770)$, we examine the invariant mass of $\gamma^H J/\psi$, where γ^H refers to the higher energetic photon in the final state $\gamma\gamma\ell^+\ell^-$. Figure 1 (a) shows the distribution of the invariant masses of $\gamma^H J/\psi$ from the Monte Carlo events of $\psi(3770) \rightarrow \gamma\chi_{cJ} \rightarrow \gamma\gamma J/\psi \rightarrow \gamma\gamma\ell^+\ell^-$, which were generated at $\sqrt{s} = 3.773$ GeV. Due to the wrong combination of the photon and J/ψ , the transition $\psi(3770) \rightarrow \gamma\chi_{c0}$ produces a broad distribution on the lower side; the events shown in the peak located at ~ 3.51 GeV/ c^2 are from the $\psi(3770) \rightarrow \gamma\chi_{c1}$ decay; while the events from the peak located at ~ 3.56 GeV/ c^2 are from the $\psi(3770) \rightarrow \gamma\chi_{c2}$ decay.

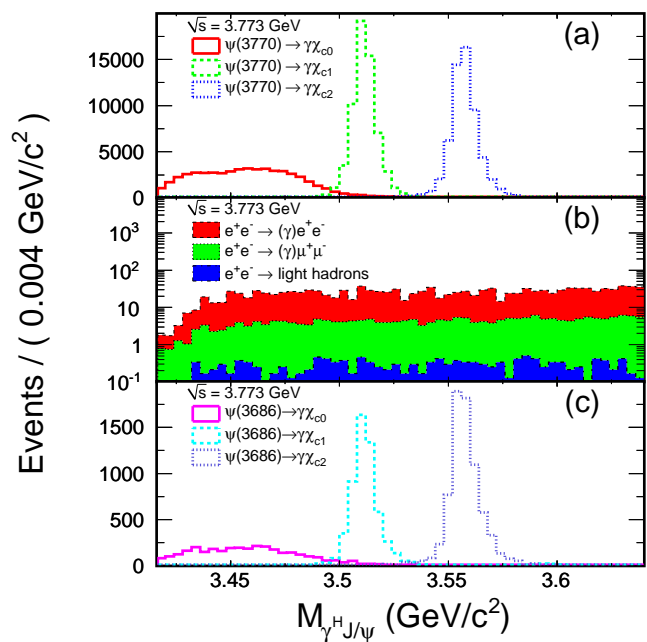


FIG. 1. Invariant mass spectra of the selected $\gamma^H J/\psi$ combinations from Monte Carlo events generated at $\sqrt{s} = 3.773$ GeV, (a) is for the events from $\psi(3770) \rightarrow \gamma\chi_{cJ} \rightarrow \gamma\gamma J/\psi \rightarrow \gamma\gamma\ell^+\ell^-$ decays, (b) is for the background events, and (c) is the $e^+e^- \rightarrow (\gamma_{\text{ISR}})\psi(3686)$, $\psi(3686) \rightarrow \gamma\chi_{cJ} \rightarrow \gamma\gamma J/\psi \rightarrow \gamma\gamma\ell^+\ell^-$ events.

Figure 2 shows the invariant-mass distribution of $\gamma^H J/\psi$ from the data. There are two clear peaks corresponding to the χ_{c1} (left) and the χ_{c2} (right) signals. Due to the small branching fraction ($\sim 1\%$) and the wrong combination of the photon and J/ψ , the events from $\chi_{c0} \rightarrow \gamma J/\psi$ decays are not clearly observed in Fig. 2.

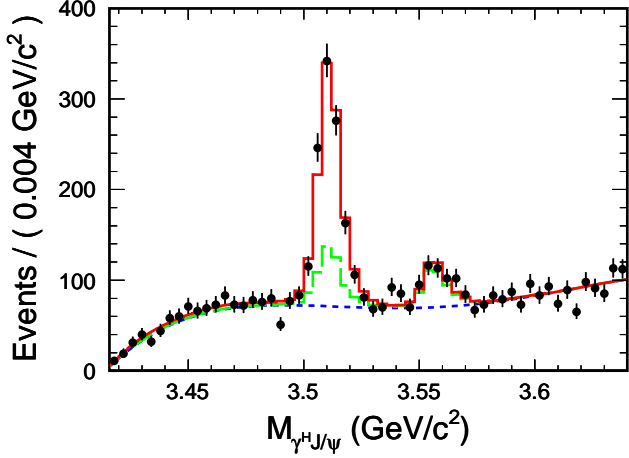


FIG. 2. Invariant mass spectrum of the $\gamma^H J/\psi$ combinations selected from data. The dots with error bars represent the data. The solid (red) line shows the fit. The dashed (blue) line shows the smooth background. The long-dashed (green) line is the sum of the smooth background and the contribution from $e^+e^- \rightarrow (\gamma_{\text{ISR}})\psi(3686)$ production.

C. Background studies

In the selected candidate events, there are both signal events for $\psi(3770) \rightarrow \gamma\chi_{cJ} \rightarrow \gamma\gamma J/\psi$ and background events. These background events originate from several sources, including (1) decays of the $\psi(3770)$ other than the signal modes in question, (2) $e^+e^- \rightarrow (\gamma)e^+e^-$, $e^+e^- \rightarrow (\gamma)\mu^+\mu^-$ and $e^+e^- \rightarrow (\gamma)\tau^+\tau^-$, where the γ in parentheses denotes the inclusion of photons from initial state radiation (ISR) and final state radiation (FSR), (3) continuum light hadron production, (4) ISR J/ψ events, (5) cross contamination between the e^+e^- and $\mu^+\mu^-$ modes of the signal events, and (6) $e^+e^- \rightarrow (\gamma_{\text{ISR}})\psi(3686)$ events produced at $\sqrt{s} = 3.773$ GeV, where the notation “ γ_{ISR} ” denotes the inclusion of produced $\psi(3686)$ due to radiative photon in the initial state.

Figure 1 (b) shows different components of the selected $\gamma\gamma J/\psi$ events misidentified from the Monte Carlo simulated background events for $e^+e^- \rightarrow (\gamma)e^+e^-$, $e^+e^- \rightarrow (\gamma)\mu^+\mu^-$, and continuum light hadron production, which are generated at $\sqrt{s} = 3.773$ GeV. The shape of the invariant-mass distribution for these background events can be well described with a polynomial function. Using MC simulation, the contributions from decays of the $\psi(3770)$ other than the signal mode, $e^+e^- \rightarrow (\gamma)\tau^+\tau^-$, ISR J/ψ events, and cross contamination between the e^+e^- and $\mu^+\mu^-$ modes of the signal events are found to be negligible.

In addition to the backgrounds described above, the background events from $e^+e^- \rightarrow (\gamma_{\text{ISR}})\psi(3686)$ with $\psi(3686) \rightarrow \gamma\chi_{cJ}$ ($\chi_{cJ} \rightarrow \gamma J/\psi$, $J/\psi \rightarrow \ell^+\ell^-$) decays can also satisfy the event selection criteria. This kind of background produced near $\sqrt{s} = 3.773$ GeV has the

same event topology as that of $\psi(3770) \rightarrow \gamma\chi_{cJ}$ decays and are indistinguishable from the signal events. The number of background events from $\psi(3686)$ decays can be estimated using

$$N_{\psi(3686) \rightarrow \gamma\chi_{cJ}} = \sigma_{\psi(3686) \rightarrow \gamma\chi_{cJ}}^{\text{obs}} \times \mathcal{L} \times \mathcal{B}_{\chi_{cJ} \rightarrow \gamma J/\psi} \times \mathcal{B}_{J/\psi \rightarrow \ell^+\ell^-} \times \eta_{\psi(3686) \rightarrow \gamma\chi_{cJ}}, \quad (1)$$

where $\sigma_{\psi(3686) \rightarrow \gamma\chi_{cJ}}^{\text{obs}}$ is the observed cross section of $e^+e^- \rightarrow \gamma_{\text{ISR}}\psi(3686)$ with $\psi(3686) \rightarrow \gamma\chi_{cJ}$ at $\sqrt{s} = 3.773$ GeV, \mathcal{L} is the integrated luminosity of the data used in the analysis, $\mathcal{B}_{\chi_{cJ} \rightarrow \gamma J/\psi}$ is the decay branching fraction of $\chi_{cJ} \rightarrow \gamma J/\psi$, $\mathcal{B}_{J/\psi \rightarrow \ell^+\ell^-}$ is the sum of branching fractions of $J/\psi \rightarrow e^+e^-$ and $J/\psi \rightarrow \mu^+\mu^-$ decays, and $\eta_{\psi(3686) \rightarrow \gamma\chi_{cJ}}$ represents the rate of misidentifying the $\psi(3686) \rightarrow \gamma\chi_{cJ}$ events as $\psi(3770) \rightarrow \gamma\chi_{cJ}$ signal events. The observed cross section for $e^+e^- \rightarrow \gamma_{\text{ISR}}\psi(3686) \rightarrow \gamma\chi_{cJ}$ at \sqrt{s} is obtained with

$$\sigma_{\psi(3686) \rightarrow \gamma\chi_{cJ}}^{\text{obs}} = \int \sigma_{\psi(3686) \rightarrow \gamma\chi_{cJ}}^{\text{D}}(s') f(s') F(x, s) G(s, s'') ds' dx, \quad (2)$$

where $\sigma_{\psi(3686) \rightarrow \gamma\chi_{cJ}}^{\text{D}}(s')$ is the dressed cross section for $\psi(3686) \rightarrow \gamma\chi_{cJ}$ decay, $s' = s(1-x)$ is the square of the actual center-of-mass energy of the e^+e^- after radiating the photons, x is the fraction of the radiative energy to the beam energy, $f(s')$ is a phase space factor, $F(x, s)$ is the sampling function for the radiative energy fraction x at \sqrt{s} [26], $G(s, s'')$ is a Gaussian function describing the distribution of the e^+e^- collision energy with an energy spread $\sigma_E = 1.37$ MeV at BEPCII. $\sigma_{\psi(3686) \rightarrow \gamma\chi_{cJ}}^{\text{D}}(s')$ is calculated with

$$\sigma_{\psi(3686) \rightarrow \gamma\chi_{cJ}}^{\text{D}}(s') = \frac{12\pi\Gamma_{\psi(3686)}^{ee}\Gamma_{\psi(3686)}^{\text{tot}}\mathcal{B}(\psi(3686) \rightarrow \gamma\chi_{cJ})}{(s'^2 - M_{\psi(3686)}^2)^2 + (\Gamma_{\psi(3686)}^{\text{tot}}M_{\psi(3686)})^2}, \quad (3)$$

where $\Gamma_{\psi(3686)}^{ee}$ and $\Gamma_{\psi(3686)}^{\text{tot}}$ are, respectively, the leptonic and total width of the $\psi(3686)$, $M_{\psi(3686)}$ is the mass of the $\psi(3686)$, and $\mathcal{B}(\psi(3686) \rightarrow \gamma\chi_{cJ})$ denotes the decay branching fraction of $\psi(3686) \rightarrow \gamma\chi_{cJ}$ ($J = 0, 1, 2$). The phase space factor is equal to [27]

$$f(s') = (E_\gamma(s')/E_\gamma^0)^3, \quad (4)$$

where $E_\gamma(s')$ and E_γ^0 are the energies of the photon in the $\psi(3686) \rightarrow \gamma\chi_{cJ}$ decay at e^+e^- energies of $\sqrt{s'}$ and $M_{\psi(3686)}$, respectively. The rates $\eta_{\psi(3686) \rightarrow \gamma\chi_{cJ}}$ of misidentifying $\psi(3686) \rightarrow \gamma\chi_{cJ}$ as $\psi(3770) \rightarrow \gamma\chi_{cJ}$ are 4.16×10^{-3} , 6.88×10^{-3} and 8.86×10^{-3} for χ_{c0} , χ_{c1} and χ_{c2} , respectively, which are estimated with Monte Carlo simulated events for $\psi(3686) \rightarrow \gamma\chi_{cJ}$ generated at $\sqrt{s} = 3.773$ GeV. With the parameters of the $\psi(3686)$ ($M_{\psi(3686)} = 3686.109_{-0.014}^{+0.012}$ MeV, $\Gamma_{\psi(3686)}^{\text{tot}} = 299 \pm 8$ keV and $\Gamma_{\psi(3686)}^{ee} = 2.36 \pm 0.04$ keV), the luminosity of the

data, the decay branching fractions and the misidentification rates, we obtain the numbers of background events from $\psi(3686) \rightarrow \gamma\chi_{cJ} \rightarrow \gamma\gamma J/\psi \rightarrow \gamma\gamma\ell^+\ell^-$ decays to be $5.3 \pm 0.3 \chi_{c0}$, $225.4 \pm 11.7 \chi_{c1}$ and $158.4 \pm 8.5 \chi_{c2}$, where the errors are mainly due to the uncertainties of the $\psi(3686)$ resonance parameters, the luminosity, the branching fractions of $\psi(3686) \rightarrow \gamma\chi_{cJ}$, $\chi_{cJ} \rightarrow \gamma J/\psi$ and $J/\psi \rightarrow \ell^+\ell^-$ decays.

D. Signal events for $\psi(3770) \rightarrow \gamma\chi_{cJ}$

To extract the number of signal events, we fit the invariant-mass spectrum of $\gamma^H J/\psi$ shown in Fig. 2 with a function describing the shape of the mass spectrum. The function is constructed with the Monte Carlo simulated signal shape as shown in Fig. 1 (a) to describe the signal, a fourth-order polynomial for the smooth background, and the Monte Carlo simulated mass shape for the $e^+e^- \rightarrow (\gamma_{\text{ISR}})\psi(3686)$ process with a yield fixed to the predicted size of the corresponding peaking background. In the fit the expected number of $\psi(3770) \rightarrow \gamma\chi_{c0}$ is fixed at 60.1 ± 8.6 events, which is estimated with the branching fraction for $\psi(3770) \rightarrow \gamma\chi_{c0}$ decay [23] and the total number of $\psi(3770)$ as well as the reconstruction efficiency. The error in the estimated number of events is from the uncertainties of the branching fractions for $\psi(3770) \rightarrow \gamma\chi_{c0}$, $\chi_{c0} \rightarrow \gamma J/\psi$ and $J/\psi \rightarrow \ell^+\ell^-$ [23], the total number of $\psi(3770)$ and the reconstruction efficiency.

The fit returns 654.2 ± 40.3 and 34.7 ± 29.4 signal events for $\psi(3770) \rightarrow \gamma\chi_{c1}$ and $\psi(3770) \rightarrow \gamma\chi_{c2}$ decays, respectively. The red solid line in Fig. 2 shows the best fit. To estimate the statistical significance of observing $\psi(3770) \rightarrow \gamma\chi_{c2}$ signal events, we perform a fit with the χ_{c2} signal amplitude fixed at zero. Transforming the ratio of the fit likelihoods into the number of standard deviations at which the null hypothesis can be excluded gives a statistical signal significance of 1.2 standard deviations.

IV. RESULT

A. Total number of $\psi(3770)$

The total number of $\psi(3770)$ produced in the data sample is given by

$$N_{\psi(3770)} = \sigma_{\psi(3770)}^{\text{obs}} \times \mathcal{L}, \quad (5)$$

where $\sigma_{\psi(3770)}^{\text{obs}}$ is the total cross section for $\psi(3770)$ production at 3.773 GeV in e^+e^- annihilation, which includes tree-level and both ISR and vacuum polarization contributions. The BES-II Collaboration previously measured the cross section $\sigma_{\psi(3770)}^{\text{obs}}(\sqrt{s})|_{\sqrt{s}=3.773 \text{ GeV}} = (7.15 \pm 0.27 \pm 0.27) \text{ nb}$ [28], which was obtained by weighting two independent measurements of this cross section [29, 30]. Using this cross section

$\sigma_{\psi(3770)}^{\text{obs}}(\sqrt{s})|_{\sqrt{s}=3.773 \text{ GeV}}$ and the luminosity of the data [16], we obtain the total number of $\psi(3770)$ produced in the data sample to be

$$N_{\psi(3770)} = (20.86 \pm 1.13) \times 10^6,$$

where the error is due to the uncertainties of the total cross section for $\psi(3770)$ production and the luminosity of the data.

B. Branching fraction

The branching fractions for $\psi(3770) \rightarrow \gamma\chi_{c1}$ and $\psi(3770) \rightarrow \gamma\chi_{c2}$ decays are determined with

$$\mathcal{B}(\psi(3770) \rightarrow \gamma\chi_{c1,2}) = \frac{N_{\psi(3770) \rightarrow \gamma\chi_{c1,2}}}{N_{\psi(3770)} \mathcal{B}_{\chi_{c1,2} \rightarrow \gamma J/\psi} \mathcal{B}_{J/\psi \rightarrow \ell^+\ell^-} \epsilon_{\psi(3770) \rightarrow \gamma\chi_{c1,2}}}, \quad (6)$$

where $N_{\psi(3770) \rightarrow \gamma\chi_{c1,2}}$ is the observed number of signal events for $\psi(3770) \rightarrow \gamma\chi_{c1,2}$ decays, $\mathcal{B}_{\chi_{c1,2} \rightarrow \gamma J/\psi}$ is the branching fraction for $\chi_{c1,2} \rightarrow \gamma J/\psi$, $\mathcal{B}_{J/\psi \rightarrow \ell^+\ell^-}$ is the branching fraction for $J/\psi \rightarrow \ell^+\ell^-$ decay, and $\epsilon_{\psi(3770) \rightarrow \gamma\chi_{c1,2}}$ is the efficiency for reconstructing this decay.

The reconstruction efficiencies for observing $\psi(3770) \rightarrow \gamma\chi_{c1}$ and $\psi(3770) \rightarrow \gamma\chi_{c2}$ decays are determined with Monte Carlo simulated events for these decays. With large Monte Carlo samples, the efficiencies are found to be $\epsilon_{\psi(3770) \rightarrow \gamma\chi_{c1}} = (31.25 \pm 0.10)\%$ and $\epsilon_{\psi(3770) \rightarrow \gamma\chi_{c2}} = (28.77 \pm 0.10)\%$, where the errors are statistical.

Inserting the corresponding numbers into Eq. (6) yields the branching fractions

$$\mathcal{B}(\psi(3770) \rightarrow \gamma\chi_{c1}) = (2.48 \pm 0.15 \pm 0.23) \times 10^{-3}, \quad (7)$$

and

$$\mathcal{B}(\psi(3770) \rightarrow \gamma\chi_{c2}) = (0.25 \pm 0.21 \pm 0.18) \times 10^{-3}, \quad (8)$$

where the first errors are statistical and the second systematic.

The systematic uncertainty in the measured branching fractions of $\psi(3770) \rightarrow \gamma\chi_{c1}$ and $\psi(3770) \rightarrow \gamma\chi_{c2}$ includes eight contributions: (1) the uncertainty in the total number of $\psi(3770)$ (5.4%), which contains the uncertainty in the observed cross section for $\psi(3770)$ production at $\sqrt{s} = 3.773 \text{ GeV}$ [28] and the uncertainty in the luminosity measurement [16], (2) the uncertainty in the particle identification (0.1%) determined by comparing the lepton identification efficiencies for data and Monte Carlo events, which are measured using the lepton samples selected from the $\psi(3686) \rightarrow \pi^+\pi^- J/\psi$, $J/\psi \rightarrow \ell^+\ell^-$ process, (3) the uncertainty in the extra $\cos\theta_{e^\pm}$ requirement (0.1%) estimated by comparing the acceptances of this requirement for data and

Monte Carlo events, which are determined using the electron samples selected from the $\psi(3686) \rightarrow \pi^+\pi^-J/\psi$, $J/\psi \rightarrow e^+e^-$ process, (4) the uncertainty due to photon selection (1.0% per photon [31]), (5) the uncertainty associated with the kinematic fit (2.1%) determined by comparing the χ^2 distributions and the efficiencies of the $\chi^2 < 25$ requirement for data and Monte Carlo simulation, which are obtained using the $\psi(3686) \rightarrow \gamma\gamma\ell^+\ell^-$ events selected from data taken at $\sqrt{s} = 3.686$ GeV and the corresponding Monte Carlo samples, (6) the uncertainty in the reconstruction efficiency (0.3%) arising from the Monte Carlo statistics, (7) the uncertainties in the branching fractions of $\chi_{c1,2} \rightarrow \gamma J/\psi$ and $J/\psi \rightarrow \ell^+\ell^-$ decays (3.6% for $\gamma\chi_{c1}$, 3.7% for $\gamma\chi_{c2}$ [23]), and (8) the uncertainty associated with the fit to the mass spectrum (6.1% for $\gamma\chi_{c1}$, 73.2% for $\gamma\chi_{c2}$) determined by changing the fitting range, changing the order of the polynomial, varying the magnitude of the peaking background from the radiative $\psi(3686)$ tail by $\pm 1\sigma$ and using an alternative signal function (Monte Carlo shape convoluted with a Gaussian function). These systematic uncertainties are summarized in Table I. Adding these systematic uncertainties in quadrature yields total systematic uncertainties of 9.4% and 73.6% for $\psi(3770) \rightarrow \gamma\chi_{c1}$ and $\psi(3770) \rightarrow \gamma\chi_{c2}$ decays, respectively.

TABLE I. Summary of the systematic uncertainties (%) in the measurements of the branching fractions for $\psi(3770) \rightarrow \gamma\chi_{c1}$ and $\gamma\chi_{c2}$.

Source	$\gamma\chi_{c1}$	$\gamma\chi_{c2}$
Total number of $\psi(3770)$	5.4	5.4
Particle identification	0.1	0.1
$\cos\theta_{e^\pm}$ cut	0.1	0.1
Photon selection	2.0	2.0
Kinematic fit	2.1	2.1
Efficiency	0.3	0.3
Branching fractions	3.6	3.7
Fit to the mass spectrum	6.1	73.2
Total	9.4	73.6

To obtain an upper limit on $\mathcal{B}(\psi(3770) \rightarrow \gamma\chi_{c2})$, we integrate a likelihood function from zero to the value of $\mathcal{B}(\psi(3770) \rightarrow \gamma\chi_{c2})$ corresponding to 90% of the integral from zero to infinity. The likelihood function is a Gaussian function constructed with the mean value of \mathcal{B} and a standard deviation which includes both the statistical and systematic errors. Using this method, an upper limit on the branching fraction of $\psi(3770) \rightarrow \gamma\chi_{c2}$ is set to

$$\mathcal{B}(\psi(3770) \rightarrow \gamma\chi_{c2}) < 0.64 \times 10^{-3} \quad (9)$$

at the 90% confidence level (C.L.).

C. Partial width

Using the total width $\Gamma_{\psi(3770)}^{\text{tot}} = (27.2 \pm 1.0)$ MeV [23], we transform the measured branching fractions to the

TABLE II. Comparison of measured partial widths with theoretical predictions, where ϕ is the mixing angle of the S - D mixing model.

Experiment/theory	$\Gamma(\psi(3770) \rightarrow \gamma\chi_{cJ})$ (keV)	
	$J = 1$	$J = 2$
This work	$67.5 \pm 4.1 \pm 6.7$	< 17.4
Ding-Qin-Chao [12]		
nonrelativistic	95	3.6
relativistic	72	3.0
Rosner S - D mixing [13]		
$\phi = 12^\circ$ [13]	73 ± 9	24 ± 4
$\phi = (10.6 \pm 1.3)^\circ$ [32]	79 ± 6	21 ± 3
$\phi = 0^\circ$ (pure 1^3D_1 state) [32]	133	4.8
Eichten-Lane-Quigg [14]		
nonrelativistic	183	3.2
with coupled-channel corr.	59	3.9
Barnes-Godfrey-Swanson [15]		
nonrelativistic	125	4.9
relativistic	77	3.3

transition widths. This yields

$$\Gamma(\psi(3770) \rightarrow \gamma\chi_{c1}) = (67.5 \pm 4.1 \pm 6.7) \text{ keV}$$

and the upper limit at the 90% C.L.

$$\Gamma(\psi(3770) \rightarrow \gamma\chi_{c2}) < 17.4 \text{ keV.}$$

The measured partial widths for these two transitions are compared to several theoretical predictions in Table II.

D. Partial cross section

Using the cross section $\sigma_{\psi(3770)} = (9.93 \pm 0.77)$ nb for $\psi(3770)$ production at $\sqrt{s} = 3.773$ GeV, which is calculated using $\psi(3770)$ resonance parameters [23], together with the measured branching fractions for these two decays, we obtain the partial cross section for the $\psi(3770) \rightarrow \gamma\chi_{c1}$ transition to be

$$\sigma(\psi(3770) \rightarrow \gamma\chi_{c1}) = (24.6 \pm 1.5 \pm 3.0) \text{ pb}$$

and the upper limit at the 90% C.L. on the partial cross section for the $\psi(3770) \rightarrow \gamma\chi_{c2}$ transition to be

$$\sigma(\psi(3770) \rightarrow \gamma\chi_{c2}) < 6.4 \text{ pb.}$$

V. SUMMARY

By analyzing 2.92 fb^{-1} of data collected at $\sqrt{s} = 3.773$ GeV with the BESIII detector operated at the BEPCII, we measure $\mathcal{B}(\psi(3770) \rightarrow \gamma\chi_{c1}) = (2.48 \pm 0.15 \pm 0.23) \times 10^{-3}$ and set a 90% C.L. upper limit $\mathcal{B}(\psi(3770) \rightarrow \gamma\chi_{c2}) < 0.64 \times 10^{-3}$. This measured branching fraction for $\psi(3770) \rightarrow \gamma\chi_{c1}$ is consistent within error with $\mathcal{B}(\psi(3770) \rightarrow \gamma\chi_{c1}) = (2.8 \pm 0.5 \pm 0.4) \times 10^{-3}$ measured by CLEO-c [10], but the precision of this measurement is improved by more than a factor of 2.

ACKNOWLEDGMENTS

The BESIII Collaboration thanks the staff of BEPCII and the IHEP computing center for their strong support. This work is supported in part by National Key Basic Research Program of China under Contracts No. 2009CB825204, and No. 2015CB856700; the National Natural Science Foundation of China (NSFC) under Contracts No. 10935007, No. 11125525, No. 11235011, No. 11322544, No. 11335008, and No. 11425524; the Chinese Academy of Sciences (CAS) Large-Scale Scientific Facility Program; the Joint Large-Scale Scientific Facility Funds of the NSFC and CAS under Contracts No. 11179007, No. U1232201, and No. U1332201; CAS under Contracts No. KJCX2-YW-N29, and No. KJCX2-

YW-N45; the 100 Talents Program of CAS; INPAC and the Shanghai Key Laboratory for Particle Physics and Cosmology; the German Research Foundation DFG under Contract No. Collaborative Research Center CRC-1044; the Istituto Nazionale di Fisica Nucleare, Italy; the Ministry of Development of Turkey under Contract No. DPT2006K-120470; the Russian Foundation for Basic Research under Contract No. 14-07-91152; the U. S. Department of Energy under Contracts No. DE-FG02-04ER41291, No. DE-FG02-05ER41374, No. DE-FG02-94ER40823, and No. DESC0010118; the U.S. National Science Foundation; the University of Groningen (RuG) and the Helmholtzzentrum fuer Schwerionenforschung GmbH (GSI), Darmstadt; and the WCU Program of the National Research Foundation of Korea under Contract No. R32-2008-000-10155-0.

-
- [1] E. Eichten, K. Gottfried, T. Kinoshita, K. D. Lane, and T.-M. Yan, *Phys. Rev. D* **17**, 3090 (1978).
- [2] E. Kou and O. Penea, *Phys. Lett. B* **631**, 164 (2005).
- [3] M. B. Voloshin, *Prog. Part. Nucl. Phys.* **61**, 455 (2008).
- [4] G. Rong, *Chin. Phys. C* **34**, 788 (2010).
- [5] J. Z. Bai *et al.* (BES Collaboration), *Chin. Phys. C* **28**, 325 (2004).
- [6] J. Z. Bai *et al.* (BES Collaboration), *Phys. Lett. B* **605**, 63 (2005).
- [7] M. Ablikim *et al.* (BES Collaboration), *Phys. Rev. Lett.* **101**, 102004 (2008).
- [8] N. E. Adam *et al.* (CLEO Collaboration), *Phys. Rev. Lett.* **96**, 082004 (2006).
- [9] R. A. Briere *et al.* (CLEO Collaboration), *Phys. Rev. D* **74**, 031106(R) (2006).
- [10] T. E. Coan *et al.* (CLEO Collaboration), *Phys. Rev. Lett.* **96**, 182002 (2006).
- [11] G. S. Adams *et al.* (CLEO Collaboration), *Phys. Rev. D* **73**, 012002 (2006).
- [12] Y.-B. Ding, D.-H. Qin and K.-T. Chao, *Phys. Rev. D* **44**, 3562 (1991).
- [13] J. L. Rosner, *Phys. Rev. D* **64**, 094002 (2001).
- [14] E. J. Eichten, K. Lane and C. Quigg, *Phys. Rev. D* **69**, 094019 (2004).
- [15] T. Barnes, S. Godfrey and E. S. Swanson, *Phys. Rev. D* **72**, 054026 (2005).
- [16] M. Ablikim *et al.* (BESIII Collaboration), *Chin. Phys. C* **37**, 123001 (2013).
- [17] M. Ablikim *et al.* (BESIII Collaboration), *Nucl. Instrum. Methods Phys. Res. Sect. A* **614**, 345 (2010).
- [18] S. Agostinelli *et al.* (GEANT4 Collaboration), *Nucl. Instrum. Methods Phys. Res., Sect. A* **506**, 250 (2003).
- [19] Z. Y. Deng *et al.*, *Chin. Phys. C* **30**, 371 (2006).
- [20] S. Jadach, B. F. L. Ward, and Z. Was, *Comput. Phys. Commun.* **130**, 260 (2000).
- [21] D. J. Lange, *Nucl. Instrum. Methods Phys. Res. Sect. A* **462**, 152 (2001); R.-G. Ping, *Chin. Phys. C* **32**, 599 (2008).
- [22] E. Eichten, K. Gottfried, T. Kinoshita, J. Kogut, K. D. Lane, and T.-M. Yan, *Phys. Rev. Lett* **34**, 369 (1975); G. Li, Y. S. Zhu and Z. Y. Wang, *Chin. Phys. C* **30**, 718 (2006).
- [23] K. A. Olive *et al.* (Particle Data Group), *Chin. Phys. C* **38**, 090001 (2014).
- [24] J. C. Chen, G. S. Huang, X. R. Qi, D. H. Zhang and Y. S. Zhu, *Phys. Rev. D* **62**, 034003 (2000).
- [25] G. Balossini, C. M. Carloni Calame, G. Montagna, O. Nicrosini and F. Piccinini, *Nucl. Phys. B* **758**, 227 (2006).
- [26] E. A. Kuraev and V. S. Fadin, *Yad. Fiz.* **41**, 733 (1985); *Sov. J. Nucl. Phys.* **41**, 466 (1985).
- [27] See Eq. (93) in N. Brambilla *et al.*, *Eur. Phys. J. C* **71**, 1534 (2011).
- [28] M. Ablikim *et al.* (BES Collaboration), *Phys. Lett. B* **650**, 111 (2007).
- [29] M. Ablikim *et al.* (BES Collaboration), *Phys. Rev. Lett.* **97**, 121801 (2006).
- [30] M. Ablikim *et al.* (BES Collaboration), *Phys. Lett. B* **652**, 238 (2007).
- [31] M. Ablikim *et al.* (BESIII Collaboration), *Phys. Rev. D* **81**, 052005 (2010).
- [32] G. Rong, D. H. Zhang, and H. L. Ma, “ $\psi(3770)$ non- $D\bar{D}$ Decays”, in *Physics at BES-III*, edited by Kuang-Ta Chao and Yifang Wang, *Int. J. Mod. Phys. A* **24** Supplement 1 (2009), p. 414.